Economic Geology, v. 100, pp. 1005–1020

Ages of Intrusion, Alteration, and Mineralization at the Grasberg Cu-Au Deposit, Papua, Indonesia

Peter J. Pollard,† Roger G. Taylor,

Economic Geology Research Unit, School of Earth Sciences, James Cook University, Townsville, Queensland 4811, Australia

and Lisa Peters

New Mexico Bureau of Mines and Mineral Resources, Socorro, New Mexico 87801

Abstract

The $^{40}Ar/^{39}Ar$ ages of 10 magmatic and hydrothermal micas from the Grasberg Igneous Complex range from 3.33 ± 0.12 to 3.01 ± 0.06 Ma. The ages of intrusive rocks and the paragenetic relationships between intrusive rocks and hydrothermal alteration and mineralization indicate that the Grasberg Igneous Complex formed during several cycles of intrusion and hydrothermal alteration. These include the Dalam and Main Grasberg intrusion and alteration cycles (3.33 ± 0.12–3.19 ± 0.05 Ma), a Kali intrusion and alteration cycle (3.16 ± 0.06–3.06 ± 0.03 Ma), and a post-Kali intrusion and Grasberg mineralization cycle (3.06 ± 0.03 and 3.01 ± 0.06 Ma). Each cycle of intrusion and alteration appears to have lasted around 0.1 m.y. or less and indicates that the huge size and high grade of Grasberg did not result from an unusually prolonged period of hydrothermal activity.

A sample of phlogopite predating magnetite from the Kucing Liar Cu-Au deposit adjacent to Grasberg has an age of 3.41 ± 0.03 Ma. This is within error of the age of a Dalam intrusive rock from the Grasberg Igneous Complex and suggests formation of the calc-silicate skarn part of Kucing Liar at an early stage in the development of the complex. The ages of the equigranular diorite from the Ertsberg intrusion (2.67 ± 0.03 Ma), phlogopite from an endoskarn vein in the intrusion (2.71 ± 0.04 Ma), and phlogopite from the Ertsberg Cu-Au deposit (2.59 ± 0.15 Ma) indicate that intrusion and alteration and/or mineralization at Ertsberg are younger than the intrusions and mineralization in the Grasberg Igneous Complex. The Ertsberg therefore represents at least one additional cycle of approximately 0.1 m.y. of intrusion and alteration and/or mineralization in the district.

The intrusions that make up the Grasberg Igneous Complex and Ertsberg and the hydrothermal fluids responsible for much of the alteration and mineralization appear to have been derived from a deeper level magma chamber. The youngest dated intrusive phase in the Grasberg Igneous Complex is a post-Kali diorite dike that is more basic than the preceding Kali quartz monzodiorite intrusions. This, together with the presence of mafic xenoliths in the Kali and Ertsberg intrusions, suggests that the magma chamber from which the intrusions and fluids were sourced was periodically replenished by basic magma. This process may also have triggered release of magma to form the shallow-level intrusions now exposed at the surface. The basic magmas also may have contributed components including fluids, metals, and/or sulfur to the Cu-Au deposits in the Ertsberg district.

Introduction

The Ertsberg district of Papua, Indonesia, contains a number of major Cu-Au deposits, including Grasberg, which is one of the world's largest porphyry Cu-Au deposits (Table 1). The huge metal inventory of Grasberg has created significant interest in the genesis of the deposit and especially the identification of particular features or processes, which may have contributed to its large size and high grade. One aspect of potential importance is the timing and duration of intrusive and hydrothermal activity, which led to the Cu-Au mineralization.

^{40}Ar-^{39}Ar dating of K-bearing minerals can be used to establish the longevity of individual magmatic-hydrothermal systems (e.g., Henry et al., 1997; Marsh et al., 1997). Results commonly indicate that intrusion-related hydrothermal systems evolve over time intervals similar to or less than the resolving power of the method, with optimal resolution possible in systems approximately 0.5 to 5 m.y. old (Marsh et al., 1997). McDowell et al. (1996) reported K-Ar ages for 15 biotite separates from intrusive rocks in the Ertsberg district, ranging from 4.4 to 2.6 Ma Recent Re-Os dating of molybdenite from Grasberg suggests that mineralization occurred at 2.88 ± 0.01

Table 1. Proven and Probable Reserves of Cu-Au Deposits in the Ertsberg District[1]

	Average ore grade			
	Ore (thousands of tonnes)	Cu (%)	Au (g/t)	Ag (g/t)
Grasberg pit	710,607	1.11	1.30	2.58
Grasberg block cave	873,792	1.00	0.76	2.82
Deep ore zone	155,243	0.92	0.63	4.98
Kucing Liar	498,999	1.30	1.18	5.61
Mill level zone	158,773	1.22	0.95	6.25
Ertsberg stockwork zone	121,714	0.49	0.90	1.65
Big Gossan	32,906	2.63	0.92	15.72
Dom block cave	43,651	1.09	0.31	5.91
Dom open pit	27,000	1.80	0.43	9.60
Total	2,796,102	1.09	0.97	3.84

[1] From Freeport-McMoRan Copper and Gold Inc. annual report (2004)

† Corresponding author: e-mail, peter.pollard@jcu.edu.au

Ma, while molybdenite from Ertsberg has an age of 2.56 ± 0.02 Ma (Mathur et al., 2005). This Pliocene age thus makes Grasberg an ideal case to examine the longevity of magmatic-hydrothermal systems leading to Cu-Au mineralization.

Recent study of the paragenesis of alteration and mineralization at Grasberg (Pollard and Taylor, 2002) provides a framework within which ^{40}Ar-^{39}Ar dating of 10 samples of intrusive and hydrothermal phases has been undertaken. In addition, two samples from the Ertsberg Igneous Complex also have been dated and one each from the Kucing Liar and Ertsberg Cu-Au deposits.

Geologic Setting

Cu-Au mineralization in the Ertsberg district is associated with Pliocene intrusive rocks that were emplaced into Cretaceous and Tertiary siliciclastic and carbonate rocks belonging mainly to the Kembelangan and New Guinea Limestone Groups (MacDonald and Arnold, 1994; Fig. 1). The diorite to quartz monzonite intrusions include the Ertsberg and Grasberg Igneous Complexes and a number of smaller bodies (Katchan, 1982; MacDonald and Arnold, 1994; McMahon, 1994a, b; Pennington and Kavalieris, 1997). Apatite fission track analysis of the intrusions has been used to suggest emplacement depths of 2 km or less (Weiland and Cloos, 1996).

In addition to the major Grasberg deposit, Cu-Au mineralization in the Ertsberg district also occurs in several skarn deposits (Fig. 1), including Ertsberg (Katchan, 1982), the Ertsberg east skarn system (Rubin and Kyle, 1998; Coutts et al., 1999), Big Gossan (Meinert et al., 1997), Kucing Liar (Widodo et al., 1999), and DOM (Mertig et al., 1994), which are distributed around the Grasberg and Ertsberg Igneous Complexes, and along major faults in the vicinity of the intrusions (Fig. 1).

The Grasberg deposit is hosted within the Grasberg Igneous Complex (Figs. 2–5), a pipelike body approximately 950 m in diameter, which flares above 3,400 m, reaching approximately 2.4 by 1.7 km at surface. Much of the Grasberg Igneous Complex is composed of brecciated igneous rocks and was referred to as the Dalam Diatreme by MacDonald and Arnold (1994), who noted that most fragments below 3,500 m are dioritic (diorite or monzodiorite porphyry), whereas those above 3,500 m are dominantly andesitic. Breccia in the upper portion of the Grasberg Igneous Complex contains blocks of volcanic debris (MacDonald and Arnold, 1994), whereas fragments composed of banded clay (Taylor, 2003) have been interpreted to be surficial lake sediments that were incorporated into the breccia in a diatreme setting (Sapiie, 1998; Prendergast, 2001). Prior to extensive mine development, part of the Grasberg Igneous Complex was overlain by remnants of a volcanic edifice that included volcaniclastic rocks and hornblende andesite flows or domes. The volcaniclastic rocks are well to poorly bedded and sorted and include tuffaceous components with eutaxitic textures and accretionary lapilli, carbonized wood fragments, and bomb and splash structures that indicate, in part, a surficial aqueous

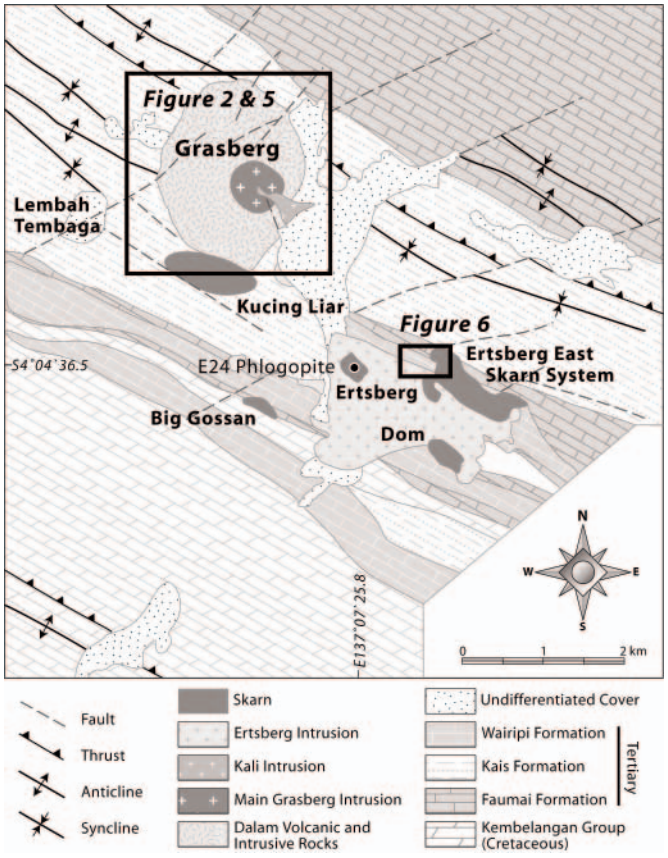

FIG. 1. Simplified surface geologic map of the Ertsberg district, showing the location of Cu-Au deposits and one of the samples dated in this study (modified from Pollard and Taylor, 2002).

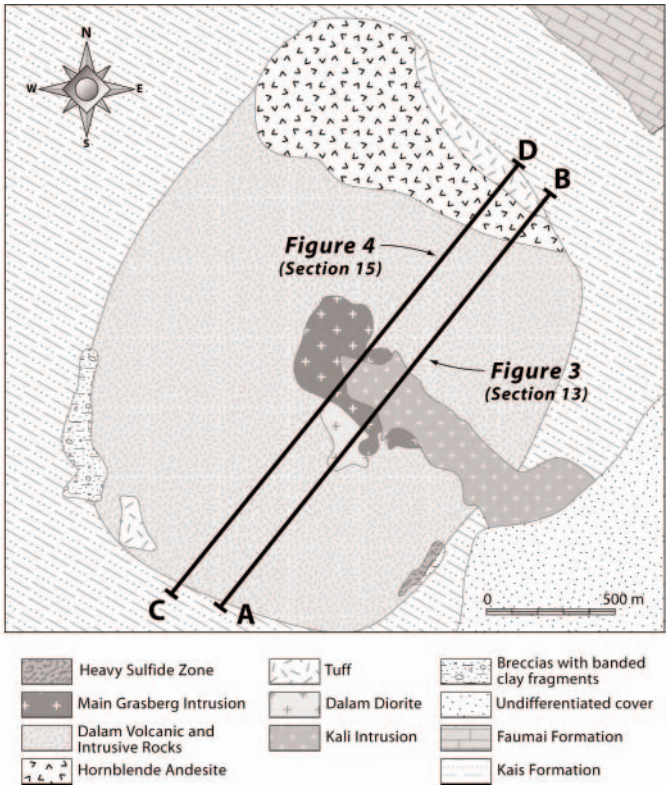

FIG. 2. Simplified geologic map of the Grasberg Intrusive Complex, showing the location of sections 13 and 15 (modified from Pollard and Taylor, 2002).

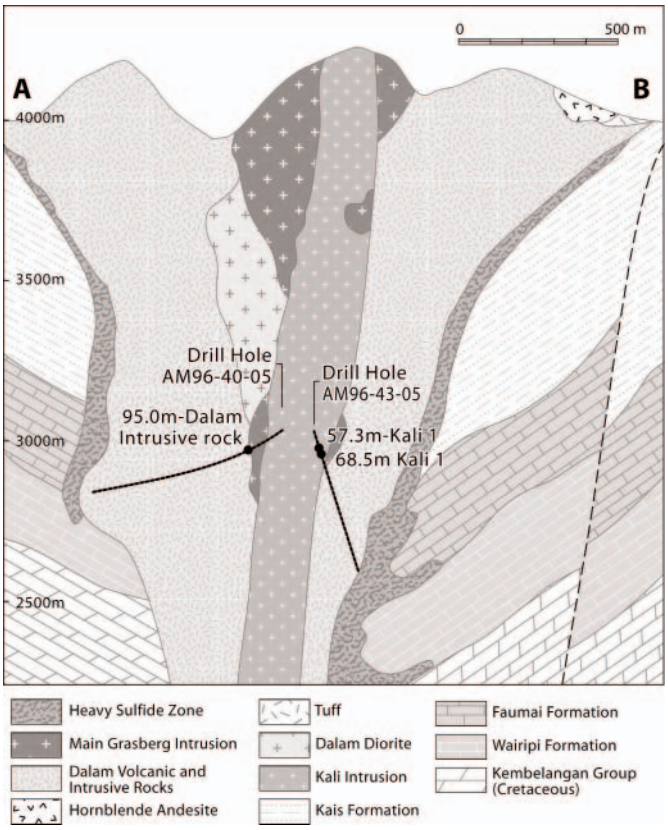

FIG. 3. Cross section 13, showing simplified geology, original surface topography, and the location of some samples dated in this study (modified from Pollard and Taylor, 2002).

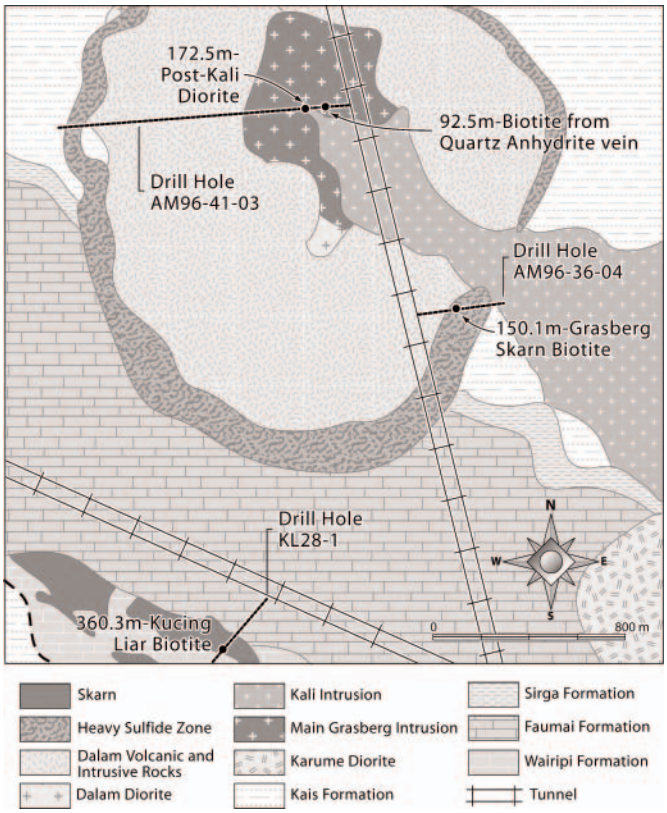

FIG. 5. Plan of the Grasberg Igneous Complex at the Amole Drift level (3,040 m), showing simplified geology and the location of samples used in this study. Note that drill hole AM96-36-04 was drilled steeply upward and the sample came from skarn apparently developed in the Kais Formation limestone (plan courtesy of P.T. Freeport Indonesia Inc.).

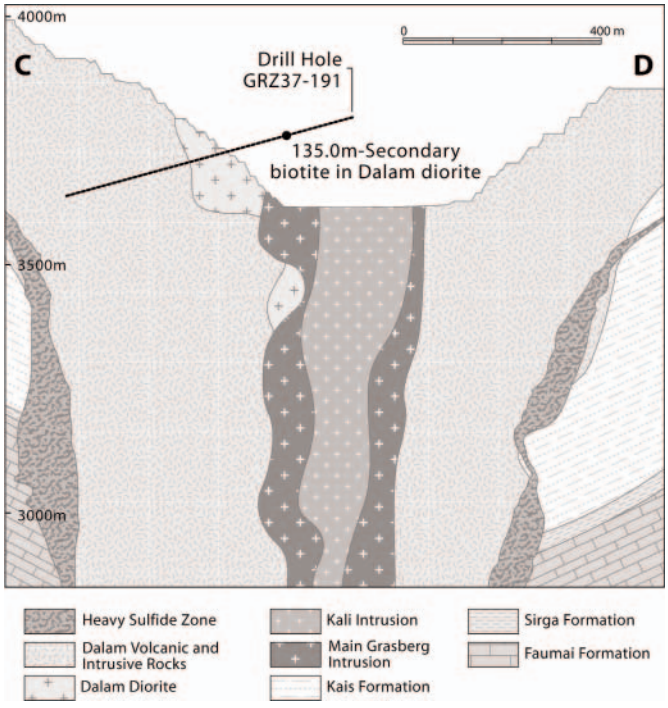

FIG. 4. Cross section 15, showing simplified geology, pit outline, and the location of a premining drill hole sampled for this study (simplified after Margotomo, 2002).

environment of deposition (MacDonald and Arnold, 1994). Pollard and Taylor (2003) suggested that breccias containing banded clay fragments and the volcanic features in the upper part of the Grasberg Igneous Complex formed late in the history of the complex. These breccias are distinct from the much earlier breccias that contain fragments of Dalam intrusive rocks and are overprinted by intensely developed potassic and other alteration as well as Cu-Au mineralization (see below).

The brecciated and strongly altered igneous rocks within the Grasberg Igneous Complex are intruded by a series of diorite to quartz monzodiorite, the identity, relative timing, and distribution of which have not been fully resolved. MacDonald and Arnold (1994) divided the intrusive rocks into three main types: (1) fine-grained diorite, which is a late dike phase of the Dalam intrusion; (2) early, middle, and late intrusions of the main Grasberg stage; and (3) early and late stages of the South Kali dike system. Pennington and Kavalieris (1997) divided the rocks that intrude the breccia pipe into (1) Dalam, (2) Grasberg, and (3) Kali quartz monzodiorites (e.g.. Fig. 3). Note that the term Dalam intrusive rocks is used here to describe the prebreccia intrusions in the Grasberg Igneous Complex, whereas Dalam diorite (Pennington and Kavalieris, 1997) is used to describe the earliest postbreccia intrusion. The Ertsberg intrusion is made up predominantly of medium-grained, equigranular diorite, which is

intruded by dikes of porphyritic diorite (Friehauf et al., 2002; Fig. 6).

Pollard and Taylor (2002) described the paragenesis of alteration and mineralization based on logging drill core from section 13, and much of the description below is summarized from that work. Our more recent work on section 15 has added a post-Kali quartz-magnetite vein stage to the paragenesis and also has resulted in revision of the timing of some sulfide stages, as discussed below and shown in Table 2.

Intrusive Rocks

Dalam intrusive rocks

The most widespread rocks within the Grasberg Igneous Complex are Dalam intrusive rocks, which are typically brecciated and severely altered in several stages (see below). Apart from several minor intrusive phases (see Pollard and Taylor, 2002), the most widespread types in section 13 are coarser and finer grained versions of a porphyritic diorite. The fine-grained porphyritic diorite contains approximately 50 percent phenocrysts of plagioclase, amphibole, and biotite in a microcrystalline matrix (Fig. 7A). A few percent of larger phenocrysts of amphibole (to 1 cm) and plagioclase (to 5 mm) occur with the predominant phenocryst population (1–2 mm). Amphibole and biotite comprise approximately 10 to 15 vol percent of the rock.

Main Grasberg intrusion

The Main Grasberg intrusion is mapped as an extensive component of the Grasberg Igneous Complex but has proven difficult to identify in drill core due to several stages of pervasive and texturally destructive alteration that includes K-feldspar, biotite, and magnetite stages. MacDonald and Arnold (1994) described the Main Grasberg stock as a medium- to coarse-grained monzodiorite porphyry containing 35 to 50 vol percent plagioclase, 2 vol percent hornblende, and 3 vol percent biotite phenocrysts.

Spatially associated with the Main Grasberg intrusion is a rare minor dike phase, known as the plagioclase dike due to the presence of prominent phenocrysts of white plagioclase (W. Margotomo, pers. commun., 2002; Fig. 7B). The plagioclase dike has a fine-grained to aphanitic matrix with <5 vol percent of plagioclase phenocrysts, typically >1 cm in length.

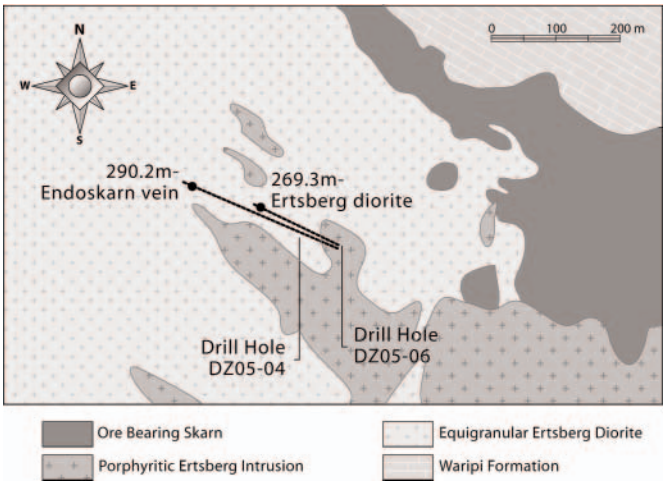

FIG. 6. Plan of part of the Ertsberg intrusion and the Ertsberg East Skarn system at the 3,289-m level (see Fig. 1), showing simplified geology and the location of samples used in this study (plan courtesy of P.T. Freeport Indonesia Inc.).

TABLE 2. Sequence of Intrusion and Alteration and/or Infilling Stages in the Grasberg Cu-Au Deposit[1]

Intrusive event	Alteration and/or vein stage
	Gypsum veins
	Pyrite veins with clay borders[2]
	Sphalerite-galena veins[2]
	Sulfur veins
	Covellite-pyrite-marcasite-sericite-chalcopyrite veins[3]
	Covellite-enargite-pyrite veins/alteration
	Quartz-carbonate veins[2]
	Mixed copper sulfide stage
	White clay-illite alteration
	Vuggy quartz veins
	Andalusite alteration
	Leaching event
	Heavy Sulfide zone pyrite
	Dark sericite-silica alteration
	Quartz-sericite alteration (silicification)
	Grasberg copper-gold veins
	Molybdenite veins
	Anhydrite-quartz veins (minor sulfides)
Post-Kali diorite	
	Chlorite veins and alteration[2]
	Amphibole veins
	Coarse-grained magnetite veins
	Biotite veins
	Quartz-magnetite veins
	Quartz veins
	Quartz veins with K-feldspar alteration borders
Kali III intrusion	
	Coarse-grained K-feldspar veins
Kali II intrusion	
	Magnetite veins (with magnetite alteration borders)
Kali I intrusion	
	MGI quartz veins
	Late K-feldspar (creamy white) alteration
	Green sericite alteration
	Brown biotite alteration
	Biotite-K-feldspar (black spot) alteration
	MGI magnetite alteration
	MGI biotite alteration
	MGI K-feldspar alteration
Main Grasberg intrusion and plagioclase dike	Dalam biotite alteration
	Dalam K-feldspar alteration
Dalam intrusive rocks	

Notes: Paragenetic position of the Dalam Diorite not defined

[1] Modified from Pollard and Taylor (2002); oldest event at the bottom with successively younger events toward the top

[2] Paragenetic position not well-constrained

[3] Could involve more than one stage

Kali intrusive rocks

Intrusive rocks in the center of the Grasberg Igneous Complex form part of the South Kali dikes and have been divided into three types by Pollard and Taylor (2002). Kali I dikes are by far the most abundant and are a fine-grained porphyritic

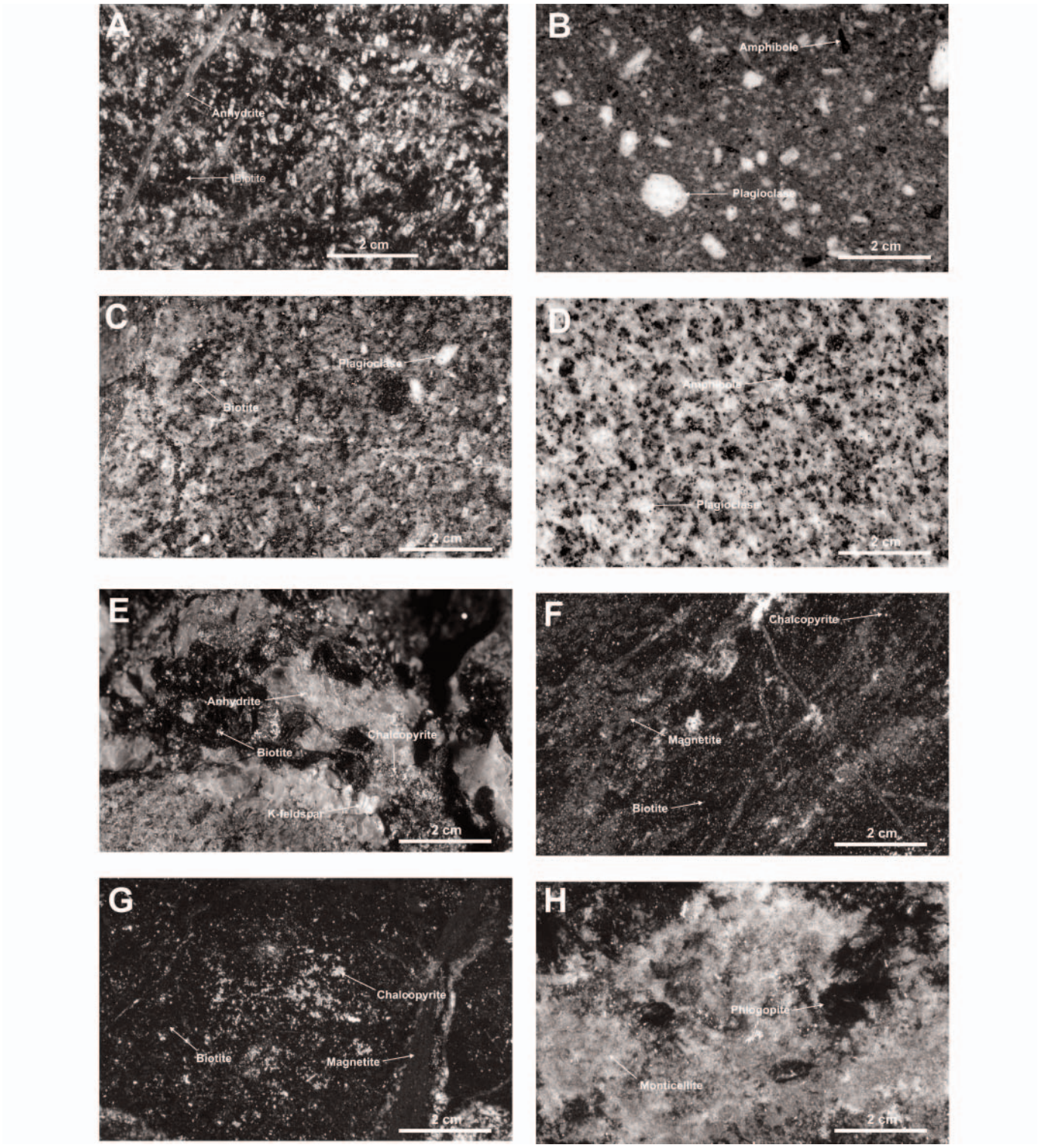

FIG. 7. Examples of intrusive rocks and hydrothermal micas from the Grasberg Igneous Complex and the Ertsberg intrusion. A. Fine-grained porphyritic diorite (Dalam intrusive rock, drill hole AM96-40-05 95.0m) with abundant plagioclase phenocrysts and intense secondary biotite alteration of the matrix. Note narrow anhydrite veins. B. Plagioclase dike (drill hole WPS3-1 313.8m) with phenocrysts of plagioclase and amphibole in a fine-grained matrix. C. Post-Kali diorite dike (drill hole AM96041-3 172.5 m) with plagioclase phenocrysts and dark secondary biotite. D. Equigranular Ertsberg diorite (drill hole DZ5-06 269.3m) with abundant amphibole and biotite. E. Anhydrite-quartz vein from the central part of Grasberg (drill hole AM96-41-3 92.5m). This part of the vein contains biotite, chalcopyrite, K-feldspar, and anhydrite infilling. F. Biotite with overprinting chalcopyrite from a skarn on the eastern side of the Grasberg Igneous Complex (drill hole AM96-36-4 150.1m). G. Biotite crosscut by magnetite vein and chalcopyrite (sample from Kucing Liar, drill hole KL28-1 360.3m, Fig. 5). H. Phlogopite overprinting monticellite from the Ertsberg Cu-Au deposit (sample E24, Fig. 1, courtesy of Gavin Clarke).

rock containing approximately 40 to 50 vol percent phenocrysts that are commonly partially aligned. The phenocryst content is variable and includes plagioclase, amphibole, biotite, clinopyroxene, magnetite, and rare quartz. Kali II dikes are a medium-grained, seriate-textured to weakly porphyritic rock, with a grain size generally <2 mm but ranging from 1 to 10 mm. Amphibole, biotite, and magnetite are the main ferromagnesian minerals and comprise 10 to 15 vol percent of the rock. The Kali II dikes occur as meter-scale intrusions that cut the Kali I dikes.

Kali III dikes are an aplitic granite (30–35 vol % quartz, 30–35 vol % K-feldspar, and 30–35 vol % plagioclase), which typically occur as centimeter- to decimeter-scale dikes that cut Kali I and Kali II dikes.

Post-Kali intrusive rocks

In drill core from the deep part of Grasberg (below approx 3,000 m, Fig. 3), an altered diorite dike has been observed crosscutting a Kali I dke (AM96-41-03, Fig. 5). A similar, less altered dike from the same hole was sampled for petrographic and geochronological study. The rock is a porphyritic microdiorite with approximately 50 vol percent phenocrysts (to 4 mm) of plagioclase and biotite with minor magnetite and apatite set in a finer grained matrix (Fig. 7C). Secondary biotite is developed at the expense of some 50 vol percent of the primary biotite, but no relicts of primary amphibole are observed. The sample is cut by minor anhydrite-quartz veins as well as minor chalcopyrite mineralization.

The lack of quartz and abundance of primary biotite in the post-Kali intrusive rock indicate that the original magma was more mafic and potassic than that from which the Kali phases crystallized, while the presence of crosscutting anhydrite-quartz veining suggests dike emplacement after the Kali dikes and associated minor vein stages but before the major anhydrite-quartz vein event.

Alteration and Cu-Au Mineralization

Dalam alteration

Pollard and Taylor (2002) noted altered fragments of Dalam intrusive rocks within an igneous matrix interpreted to be the Main Grasberg intrusion. This suggested that the K-feldspar and biotite alteration within the fragments of Dalam intrusive rock were pre-Main Grasberg intrusion in timing. The clasts of Dalam intrusive rocks are partly altered to pale brown, texturally destructive, and fracture-controlled K-feldspar alteration. Dalam K-feldspar alteration is overprinted by dark, fine-grained biotite (Fig. 7A). This varies considerably in intensity and in hand specimen ranges from veinlets to irregular blotches and zones of fine-grained dark rock.

Main Grasberg intrusion alteration

Secondary K-feldspar occurs as irregularly distributed alteration of the igneous matrix of the Main Grasberg intrusion and, in more intensely altered samples, also has replaced the phenocrysts and destroyed the original texture of the rock. Secondary biotite occurs as discontinuous veins and as relatively coarse grained clusters interpreted as replacements of mafic phenocrysts. Within the altered porphyry matrix, biotite occurs as micron-scale crystals that occur as vaguely spotted zones and selective replacements of feldspar phenocrysts. Secondary magnetite is mainly present as fine-grained alteration of igneous rocks and earlier alteration styles adjacent to numerous millimeter-scale cracks. The magnetite crystals are variably altered to hematite along internal fractures and grain boundaries.

Other post-Main Grasberg intrusion and pre-Kali stages

A biotite-K-feldspar vein infilling and alteration stage is widespread throughout the central to inner zone of the Grasberg Igneous Complex. It is distinguished by the presence of coarse-grained dark biotite and finer grained, pale pink to cream feldspar. Brown biotite alteration also affected extensive zones within the central to outer sections of the Grasberg Igneous Complex, particularly below 3,000 m. All the original mafic minerals (including primary and secondary biotite) have been converted to brown biotite, giving the rocks a dull brownish color.

Green-gray, fine-grained sericite alteration is most noticeable in Dalam intrusive rocks where it has overprinted rocks that were previously altered to fine-grained K-feldspar and weak biotite alteration. Late K-feldspar alteration is widespread and extremely texturally destructive. The alteration is commonly pale gray-white to cream, in some cases with a pink tint. This alteration has overprinted the biotite-K-feldspar alteration and, therefore, is post-Main Grasberg intrusion.

Quartz veins associated with the Main Grasberg intrusion stage are one of the most spectacular features of the Grasberg system and, although barren, are abundant and formed over a vertical extent of 1,600 to 2,000 m (Pollard and Taylor, 2002). The veins are commonly less than 10 cm wide, although examples >1 m have been observed on the southeastern side of the Grasberg Igneous Complex. The veins appear monomineralic in hand specimen, being composed solely of quartz, mostly with no visible alteration halos. The veins are commonly fractured along their margins, central zones and/or randomly, and these fractures may contain magnetite, biotite, anhydrite, bornite, chalcopyrite, pyrite, and other hydrothermal minerals. This commonly gives a false impression that minerals other than quartz were part of the quartz vein stage.

Post-Kali alteration

A series of very minor vein stages is present within and around the Kali intrusive rocks and, with the exception of fine-grained magnetite, have overprinted all Kali intrusions. Fine-grained magnetite alteration occurs sporadically within and adjacent to Kali I intrusions as oriented crackle zones. These zones are cut by the Kali II and Kali III intrusions.

Coarse-grained K-feldspar veins occur in the vicinity of the fine-grained leucocratic dikes (Kali III) as part of an aplite-pegmatite association. Quartz veins with white K-feldspar alteration borders are common in and adjacent to the Kali intrusive rocks in the deep part of the Grasberg deposit. A late quartz-magnetite vein stage was recognized during recent work on section 15 and also was mapped in the Grasberg pit by Pennington and Kavalieris (1997). The veins commonly consist of alternating bands of quartz and magnetite that

appear to be dominantly infilling phases. Up to eight cycles of alternating quartz and magnetite have been observed, and the veins are cut by minor quartz veins.

Biotite veins (1–2 mm thick) occur throughout the Kali zone and are conspicuous because the drill core commonly breaks along the veins. There is also a third stage of magnetite-bearing veins (0.1–0.2 cm wide) which is distinctive because the veins contain only magnetite and have little or no visible alteration halo. Amphibole also occurs in narrow (0.2–1 cm) veins with no apparent associated alteration.

Grasberg mineralization

Abundant anhydrite-quartz veins with K-feldspar, biotite, amphibole, apatite, chalcopyrite, bornite, and pyrite (e.g., Fig. 7E) occur in the deep part of Grasberg (below 3,000 m) and extend from the central Kali intrusions toward the outer edges of the Grasberg Igneous Complex. Veins are generally 0.5 to 4 cm wide and are identified by the presence of lilac/pale purple anhydrite. The quartz component is distinctive as coarsely granular to comb textured and white in color and can generally be distinguished from the finer, gray-colored quartz of the Main Grasberg intrusion veins.

Molybdenite veins are characteristically narrow (1 mm) and composed solely of molybdenite. The veins commonly occur along the margins of anhydrite-quartz veins and in other cases cut these veins. Based on our logging to date, molybdenite veins are more prominent in the deep part of Grasberg (below 3,000 m, Pollard and Taylor, 2002).

Chalcopyrite-bornite veins account for the bulk of the copper and gold in the Grasberg deposit. Detailed drill core logging of their distribution (Pollard and Taylor, 2002) indicates that the veins are concentrated adjacent to the Kali intrusions, with a lower vein density in the Kali intrusions and toward the perimeter of the Grasberg Igneous Complex. As the chalcopyrite-bornite veins overprint the Kali intrusions, this distribution pattern is interpreted to indicate that contact between the Kali intrusions and older intrusive rocks may have been a major control on the distribution of the veins. The chalcopyrite-bornite veins are generally less than 0.5 cm wide and are composed dominantly of chalcopyrite and bornite, with native gold, hematite, and locally minor quartz. Sulfide alteration spots are also widely developed, particularly in original mafic minerals in the intrusive rocks and within zones of earlier biotite and K-feldspar alteration. The veins commonly exploit preexisting quartz veins which have been fractured along their centerlines.

We now group the major episode of chalcopyrite-bornite mineralization at Grasberg with the anhydrite-quartz veins and molybdenite veins rather than with the heavy sulfide zone (see Pollard and Taylor, 2002). Pyrite veins believed to be equivalent to heavy sulfide zone pyrite have been observed to cut molybdenite veins and chalcopyrite veins, suggesting that the heavy sulfide zone pyrite (and the spatially associated quartz ± sericite and dark sericite-silica alteration stages: Pollard and Taylor, 2002) are later than the major chalcopyrite-bornite mineralization. Rare chalcopyrite-bornite veins that have been observed to cut the heavy sulfide zone are now considered to be part of the mixed copper sulfide stage (see below).

Heavy sulfide zone

The northeast part of Grasberg below 3,000 m contains a zone of quartz veining linked to intense silica alteration of preexisting wall rocks. Drill core intersections of 100 m or more consist of fine-grained gray-white quartz with veins up to 5 cm wide. Dark, fine-grained sericite-silica alteration is prominent in the outer parts of Grasberg below 3,000 m. The sericitization postdates previous feldspathization and silicification of original porphyritic igneous rocks and is overprinted by pyrite of the heavy sulfide zone.

The heavy sulfide zone occurs mainly near the margin of the Grasberg Igneous Complex (Figs. 3–5) and consists of zones of massive, fine-grained replacement pyrite grading into veins with less well-developed alteration in peripheral zones. Pyrite replaces carbonate and silicified-, sericitized-, feldspathized- and magnetite-altered intrusive rocks. The pyrite contains minor amounts of intergranular chalcopyrite and one gold grain was observed in the pyrite during this study.

The relationships between pyrite of the heavy sulfide zone and andalusite alteration, acid leaching, and illite alteration of the high-sulfidation system (see below) are not well established because no clear crosscutting relationships have been observed in the areas studied in detail.

High-sulfidation Cu-rich mineralization

Andalusite ± rare corundum occurs mainly as an alteration of feldspar phenocrysts in the intrusive rocks in the deeper parts of the Grasberg deposit. The major occurrences are associated with the development of white sericitic-argillic alteration zones and vuggy quartz veins interpreted as quartz-anhydrite veins from which the anhydrite has been leached.

The mixed copper-sulfide stage is composed largely of chalcopyrite, bornite, nukundamite ($Cu_{3.37}$, $Fe_{0.66}$ $S_{3.97}$: Rice et al., 1979), digenite-chalcocite, covellite, and pyrite and commonly occurs within sericitic-argillic altered rocks. The sulfides occur in discontinuous veins and in cavities partially lined by crystalline quartz that has been overgrown by late muscovite crystals. Molybdenite, chalcopyrite, nukundamite, pyrite, covellite, and minor valleriite [4(Fe, Cu)S·3(Mg, Al)(OH_2)] occur in cavities, with additional late covellite in cracks traversing earlier formed minerals.

Covellite occurs in the outer parts of the Grasberg Igneous Complex where the most common occurrence is as millimeter-scale veins, some of which also contain enargite (see Pollard and Taylor, 2002). The veins occur in and around zones dominated by pyrite veins and massive pyrite of the heavy sulfide zone. The covellite-pyrite-marcasite-sericite-chalcopyrite stage is poorly defined and includes a series of isolated occurrences that postdate the mixed copper sulfide stage. Several stages could be present and/or some examples may link with the earlier mixed copper sulfide and covellite-enargite-pyrite stages.

Native sulfur occurs as infilling within discontinuous narrow zones (1–2 cm wide), and as late-stage infilling within vugs of fine-grained pyrite-marcasite-covellite. The occurrence as isolated veins without sulfides suggests that sulfur is a separate stage, and the post-covellite timing suggests that it is very late.

Samples and Methodology

Samples

Ten samples from the Grasberg Igneous Complex, one from Kucing Liar, and three from the Ertsberg Igneous Complex and associated mineralization have been dated using the $^{40}Ar/^{39}Ar$ technique. Samples from the Grasberg Igneous Complex include primary ± secondary biotite from six intrusive rocks, three samples of hydrothermal biotite, and one sample of hydrothermal amphibole. The intrusive rocks comprise, from oldest to youngest in crosscutting sequence, samples of Dalam intrusive rock (AM96-40-05 95.0m; Fig. 7A), plagioclase dike (AM96-50-05 12.5m; Fig. 7B), two samples of Kali I intrusive rock (AM96-43-5 57.3 m and AM96-43-5 68.5m), Kali II intrusive rock (AM96-56-1 375m), and a post-Kali diorite dike (AM96-41-3 172.5m, Fig. 7C). Due to the shallow level of emplacement and small volumes of intrusive rocks in the Ertsberg district it is inferred that they cooled rapidly and therefore that the ages of primary and secondary biotite should closely approximate the time of crystallization of the host intrusion and subsequent hydrothermal alteration (see also McDowell et al., 1996).

Other samples dated here include biotite from a quartz-anhydrite vein (AM96-41-3 92.5m; Fig. 7E), secondary biotite in the Dalam diorite (GRZ37-191 135m), and biotite from a skarn on the eastern side of the Grasberg Igneous Complex (AM96-36-4 150.1m; Fig. 7F). One sample of hydrothermal actinolite was taken from a quartz-anhydrite vein (AM96-41-3 53.5m). A sample of phlogopite from the Kucing Liar Cu-Au deposit (KL28-1 360.3m; Fig. 7G) also was analyzed. The phlogopite forms part of an early silicate skarn assemblage and is overprinted by magnetite that predated sulfide mineralization. The Kucing Liar deposit is described by Widodo et al. (1999).

Samples analyzed from the Ertsberg Igneous Complex comprise one sample of magmatic biotite from equigranular Ertsberg diorite (DZ5-06 269.3m; Figs. 6, 7D), which is the major intrusive phase, and one sample of phlogopite from an endoskarn vein (DZ5-04 290.2m; Fig. 6). A sample of phlogopite from skarn in the open pit of the Ertsberg Cu-Au deposit (Katchan, 1982; Clarke, 2003; Figs. 1, 7H) also was analyzed.

Isotopic analysis and results

Nine of the samples were analyzed by step heating in an Mo double-vacuum resistance furnace, and five were analyzed by step heating using a 50-W CO_2 laser equipped with a beam integrator lens at the New Mexico Bureau of Mines and Mineral Resources. More detailed information on the analytical methods and instrumentation is included the Appendix. Eight samples (AM96-41-3 92.5 m, KL28-1 360.3m, DZ5-04 290.2m, AM96-41-3 172.5m, AM96-40-5 95.0m, AM96-56-1 375m, AM96-50-05 12.5m, and GRZ37-191 135m) yielded well-behaved age spectra (Fig. 8). Weighted mean ages have been calculated for >58 percent of the ^{39}Ar released during heating (Table 3). Inverse isochron analysis of these samples yields trapped initial $^{40}Ar/^{36}Ar$ compositions within error of the atmospheric value (Table 3, Fig. 8). The weighted mean ages calculated from the age spectra have been assigned as the preferred ages of these samples and represent the time at which the samples cooled through the blocking temperature for Ar diffusion (300°–350°C for biotite: McDougall and Harrison, 1999).

Six samples (AM96-41-3 53.3m, AM96-43-5 57.3m, AM96-43-5 68.5m, AM96-36-4 150.1m, and DZ5-06 269.3m, E24) had spectra with increasing radiogenic yields over the initial heating steps that are correlated with decreasing apparent ages. This relationship suggests the presence of excess Ar. Inverse isochron analysis confirms this, as initial $^{40}Ar/^{36}Ar$ ratios of the trapped argon are above the atmospheric value (Table 3, Fig. 8). The isochron ages are assigned as the preferred ages of these samples.

Interpretation of $^{40}Ar/^{39}Ar$ Results

The dated intrusive rocks have ages consistent with observed field relationships and range between 3.33 ± 0.12 and 3.06 ± 0.03 Ma (Table 3, Fig. 9). The Dalam intrusive rock is the oldest and provides a minimum age for the Dalam intrusive rocks and associated K-feldspar and biotite alteration. The age of the plagioclase dike (3.19 ± 0.05 Ma) provides a younger age limit for the Main Grasberg intrusion and the associated alteration and vein stages. This includes the major Main Grasberg intrusion quartz vein stockwork system because the plagioclase dike contains quartz vein fragments interpreted to be derived from the Main Grasberg intrusion quartz veins (Margotomo, 2002).

The two dated samples of Kali I intrusive rocks have ages of 3.16 ± 0.06 and 3.12 ± 0.04 Ma (Table 3, Fig. 9), which are similar to K-Ar ages of 3.14 ± 0.08 and 3.13 ± 0.15 Ma reported by McDowell et al. (1996). A sample of Kali II intrusive rock from southeast Grasberg (AM96-56-1 375 m) has an age of 3.09 ± 0.03 Ma (Table 3, Fig. 9), consistent with the observation that Kali II dikes cut Kali I dikes. The post-Kali diorite dike from drill hole AM96-41-3 172.5m (Fig. 5) has an age of 3.06 ± 0.03 Ma and is the youngest dated intrusive rock from the Grasberg Igneous Complex (Table 3, Fig. 9). This provides a minimum age for the post-Kali alteration stages and a maximum age for Grasberg Cu-Au mineralization.

Biotite from the major quartz-anhydrite vein system that overprints Kali intrusions and the associated minor vein stages has an age of 3.07 ± 0.01 Ma, whereas amphibole from the same vein stage has an age of 3.13 ± 0.23 Ma (Table 3, Fig. 9).

Biotite from a skarn at the eastern margin of the Grasberg Igneous Complex (AM96-36-4 150.1m; Fig. 5) has an age of 3.01 ± 0.06 Ma (Table 3, Fig. 9) and is cut by chalcopyrite veins and partially replaced by chalcopyrite that is interpreted to be part of the Grasberg chalcopyrite-bornite vein system. A sample of secondary biotite from core logged as Dalam diorite (GRZ37-191 135m; Fig. 4) has an age of 3.02 ± 0.03 Ma, similar to the age of the skarn biotite (Table 3, Fig. 9) and may be related to the same alteration event.

Phlogopite from the Kucing Liar Cu-Au deposit (KL28-1 360.3m; Figs. 5, 7G) has an age of 3.41 ± 0.03 Ma. This result is interpreted to indicate that formation of the Kucing Liar skarn occurred early in the history of the Grasberg Igneous Complex. The age of the phlogopite is within error of the age of secondary biotite alteration in the fine-grained Dalam intrusion (3.33 ± 0.12 Ma), and it is therefore possible that these two hydrothermal events were linked (i.e.,

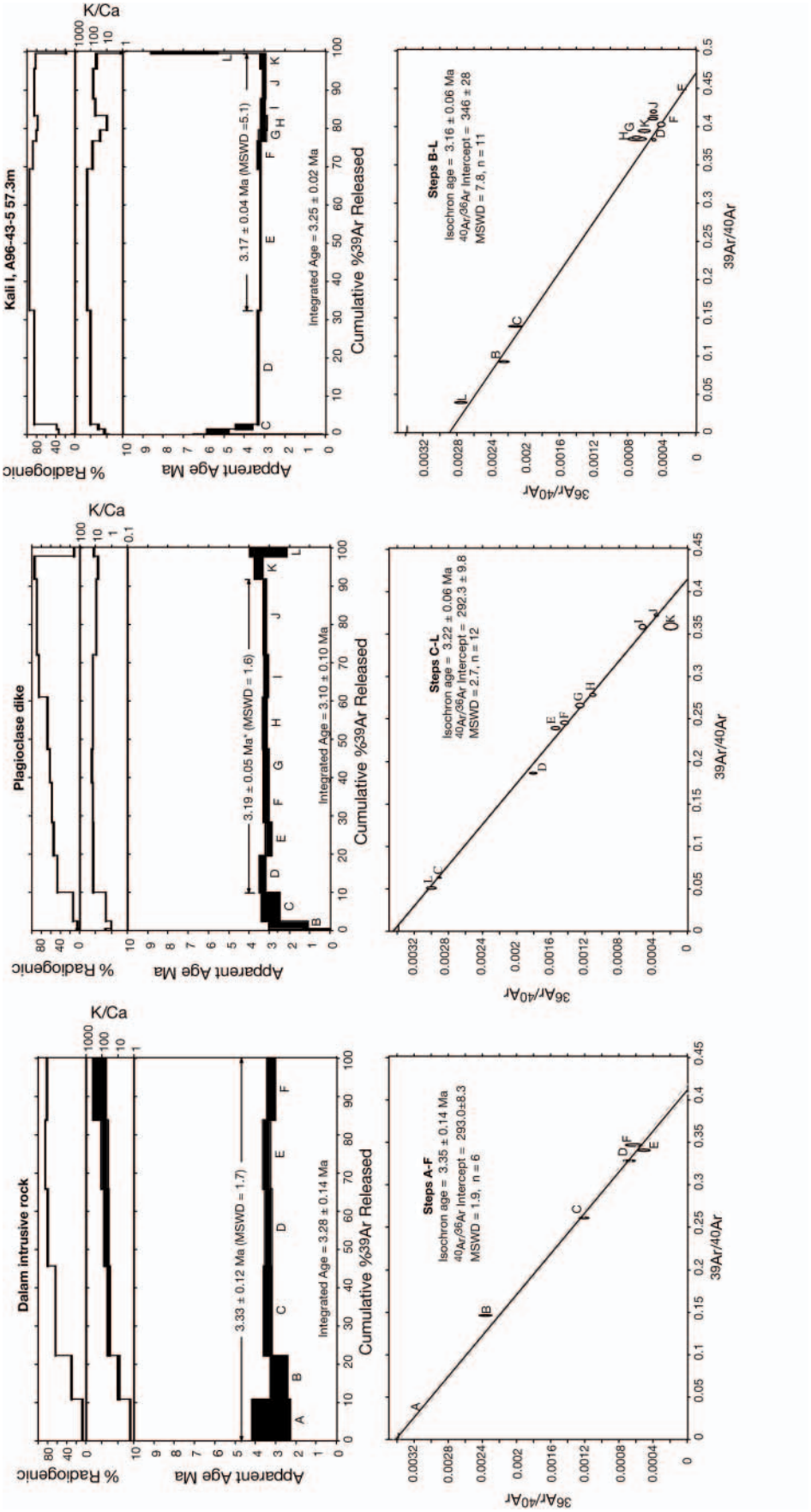

FIG. 8. $^{40}Ar/^{39}Ar$ apparent age spectra and $^{36}Ar/^{40}Ar$ vs. $^{39}Ar/^{40}Ar$ isochron diagrams for samples from the Ertsberg district.

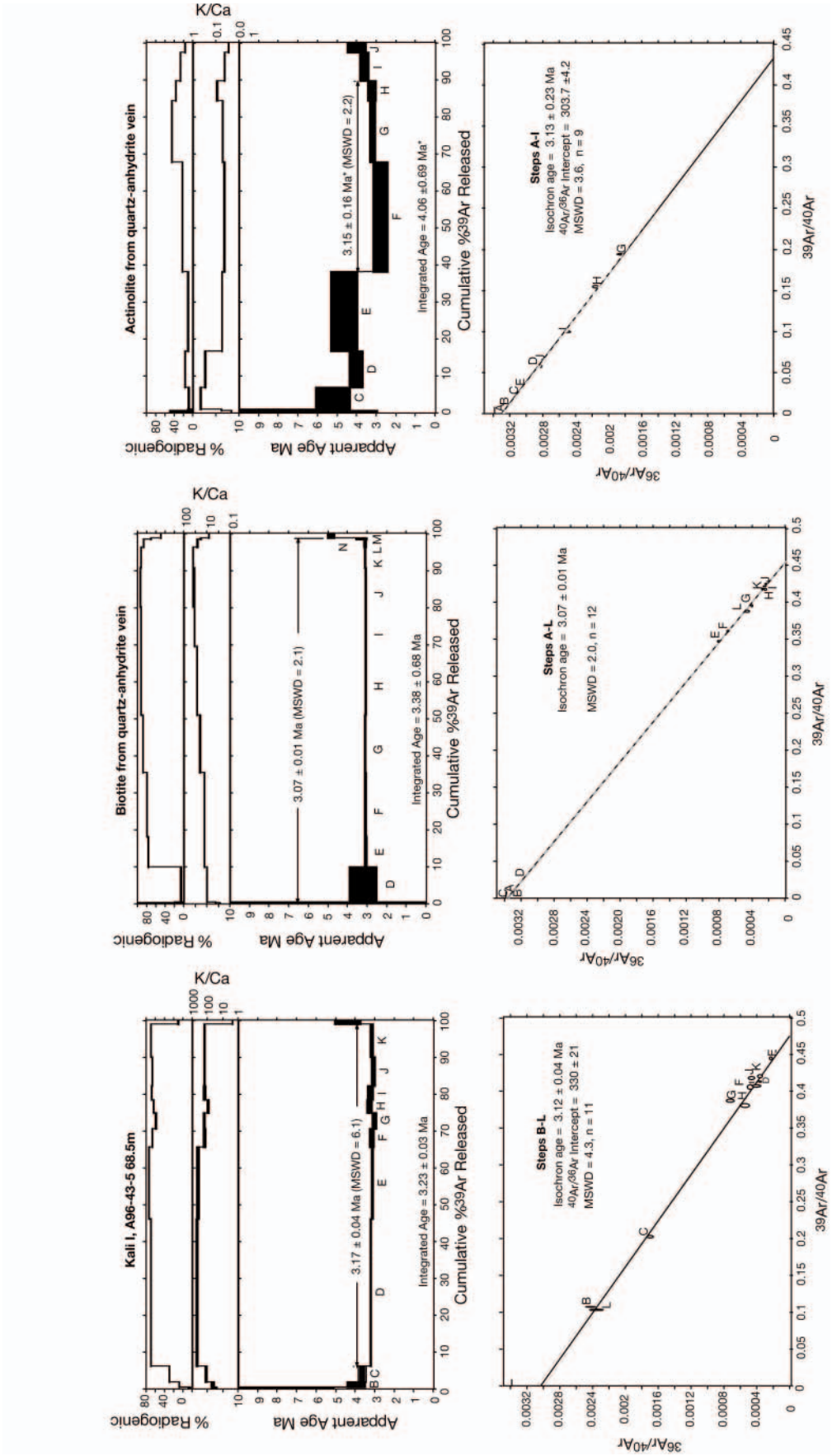
Actinolite from quartz-anhydrite vein
K/Ca
% Radiogenic
Apparent Age Ma
3.15 ± 0.16 Ma* (MSWD = 2.2)
Integrated Age = 4.06 ±0.69 Ma*
Cumulative %39Ar Released
Steps A-I
Isochron age = 3.13 ± 0.23 Ma
40Ar/36Ar Intercept = 303.7 ±4.2
MSWD = 3.6, n = 9
36Ar/40Ar
39Ar/40Ar
Biotite from quartz-anhydrite vein
3.07 ± 0.01 Ma (MSWD = 2.1)
Integrated Age = 3.38 ± 0.68 Ma
Steps A-L
Isochron age = 3.07 ± 0.01 Ma
MSWD = 2.0, n = 12
Kali I, A96-43-5 68.5m
3.17 ± 0.04 Ma (MSWD = 6.1)
Integrated Age = 3.23 ± 0.03 Ma
Steps B-L
Isochron age = 3.12 ± 0.04 Ma
40Ar/36Ar Intercept = 330 ± 21
MSWD = 4.3, n = 11

FIG. 8. *(Cont.)*

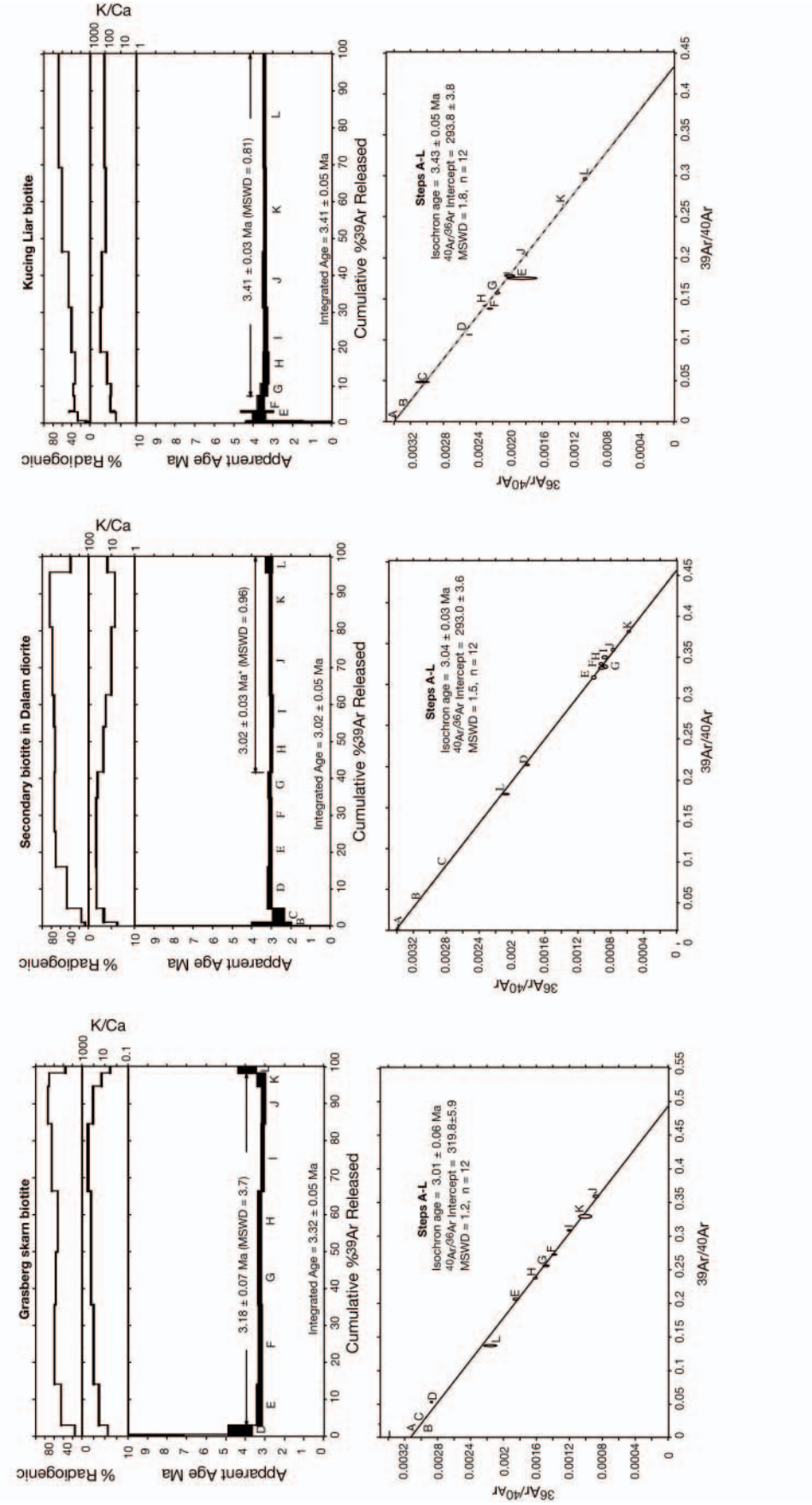
Kucing Liar biotite
Secondary biotite in Dalam diorite
Grasberg skarn biotite
K/Ca
% Radiogenic
Apparent Age Ma
Cumulative %39Ar Released
Integrated Age = 3.41 ± 0.05 Ma
3.41 ± 0.03 Ma (MSWD = 0.81)
Integrated Age = 3.02 ± 0.05 Ma
3.02 ± 0.03 Ma* (MSWD = 0.96)
Integrated Age = 3.32 ± 0.05 Ma
3.18 ± 0.07 Ma (MSWD = 3.7)
Steps A-L
Isochron age = 3.43 ± 0.05 Ma
40Ar/36Ar Intercept = 293.8 ± 3.8
MSWD = 1.8, n = 12
Isochron age = 3.04 ± 0.03 Ma
40Ar/36Ar Intercept = 293.0 ± 3.6
MSWD = 1.5, n = 12
Isochron age = 3.01 ± 0.06 Ma
40Ar/36Ar Intercept = 319.8±5.9
MSWD = 1.2, n = 12
36Ar/40Ar
39Ar/40Ar

FIG. 8. *(Cont.)*

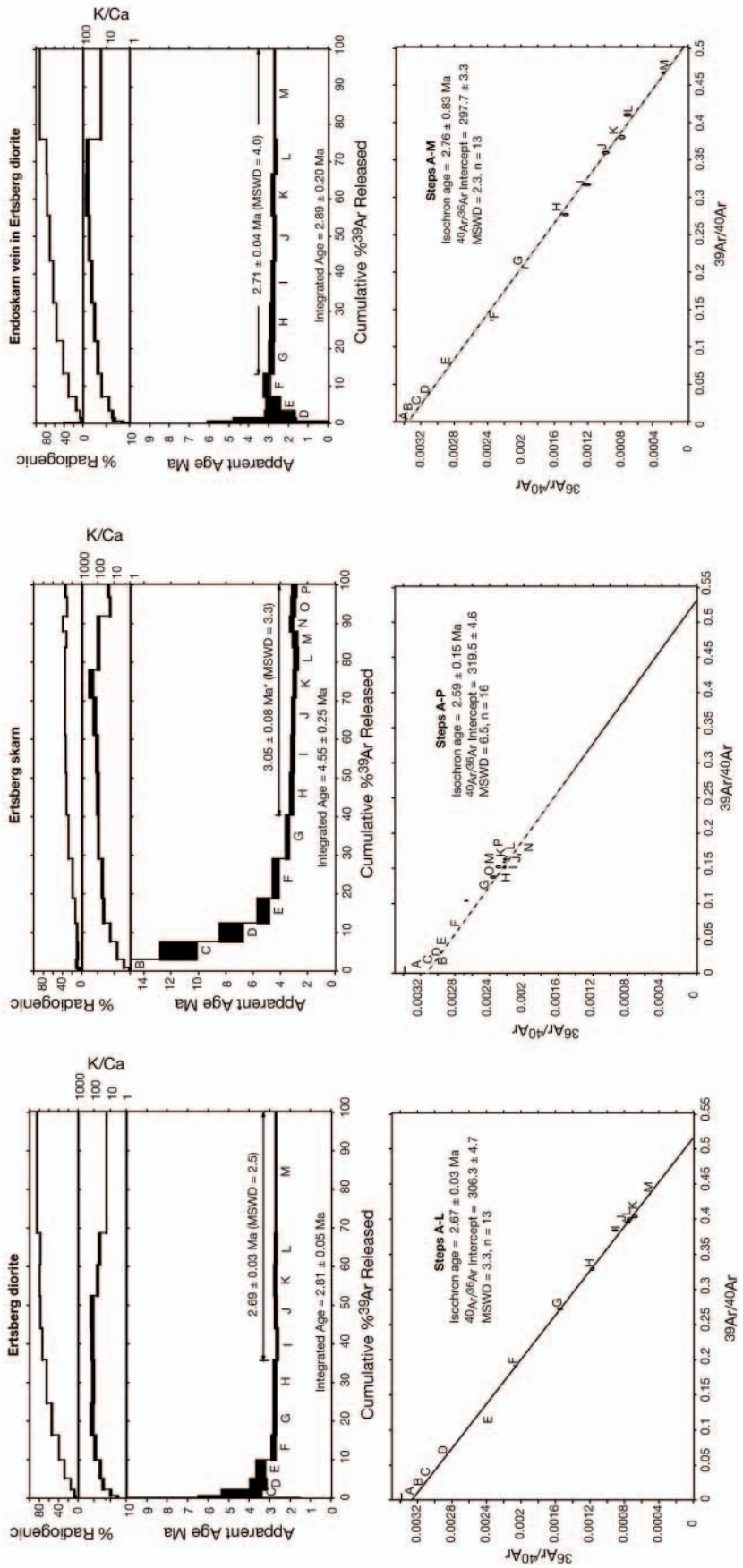
Endoskarn vein in Ertsberg diorite
K/Ca
% Radiogenic
Apparent Age Ma
2.71 ± 0.04 Ma (MSWD = 4.0)
Integrated Age = 2.89 ± 0.20 Ma
Cumulative %39Ar Released
Steps A-M
Isochron age = 2.76 ± 0.83 Ma
40Ar/36Ar Intercept = 297.7 ± 3.3
MSWD = 2.3, n = 13
36Ar/40Ar
39Ar/40Ar
Ertsberg skarn
3.05 ± 0.08 Ma* (MSWD = 3.3)
Integrated Age = 4.55 ± 0.25 Ma
Steps A-P
Isochron age = 2.59 ± 0.15 Ma
40Ar/36Ar Intercept = 319.5 ± 4.6
MSWD = 6.5, n = 16
Ertsberg diorite
2.69 ± 0.03 Ma (MSWD = 2.5)
Integrated Age = 2.81 ± 0.05 Ma
Steps A-L
Isochron age = 2.67 ± 0.03 Ma
40Ar/36Ar Intercept = 306.3 ± 4.7
MSWD = 3.3, n = 13

FIG. 8. *(Cont.)*

TABLE 3. Summary of $^{40}Ar/^{39}Ar$ Data and Analytical Methods

Sample	Description	Irradiation	Mineral	Analysis	No. of steps	MSWD[1]	Age	±2σ	Comments
AM96-41-3 92.5m	Quartz-anhydrite vein	NM-98	Biotite	Furnace step-heat	13	2.1	3.07	0.01	Age spectrum, preferred age
AM96-41-3 53.5m	Quartz-anhydrite vein	NM-98	Actinolite	Furnace step-heat	9	3.6	3.13	0.23	Isochron, preferred age
AM96-43-5 57.3m	Kali I intrusion	NM-115	Biotite	Furnace step-heat	11	7.8	3.16	0.06	Isochron, preferred age
AM96-43-5 68.5m	Kali I intrusion	NM-115	Biotite	Furnace step-heat	11	4.3	3.12	0.04	Isochron, preferred age
KL28-1 360.3m	Kucing Liar	NM-115	Phlogopite	Furnace step-heat	6	0.81	3.41	0.03	Age spectrum, preferred age
AM96-36-4 150.1m	Grasberg skarn	NM-115	Biotite	Furnace step-heat	12	1.2	3.01	0.06	Isochron, preferred age
DZ5-06 269.3m	Ertsberg diorite	NM-123	Biotite	Laser step-heat	12	3.3	2.67	0.03	Isochron, preferred age
E24	Ertsberg skarn	NM-123	Phlogopite	Laser step-heat	12	6.5	2.59	0.15	Isochron, preferred age
DZ5-04 290.2m	Endoskarn vein in Ertsberg diorite	NM-123	Biotite	Laser step-heat	7	4.0	2.71	0.04	Age spectrum, preferred age
AM96-41-3 172.5m	Post-Kali diorite	NM-123	Biotite	Laser step-heat	10	4.3	3.06	0.03	Age spectrum, preferred age
AM96-40-5 95.0m	Dalam intrusive rock	NM-123	Biotite	Laser step-heat	6	1.7	3.33	0.12	Age spectrum, preferred age
AM96-56-1 375m	Kali II intrusion	NM-133	Biotite	Furnace step-heat	7	2.3	3.09	0.03	Age spectrum, preferred age
AM96-50-05 12.5m	Plagioclase dyke	NM-148	Biotite	Furnace step-heat	7	1.6	3.19	0.05	Age spectrum, preferred age
GRZ37-191 135m	Dalam diorite	NM-148	Biotite	Furnace step-heat	5	0.96	3.02	0.03	Age spectrum, preferred age

[1] MSWD outside 95 percent confidence interval

FIG. 9. Summary diagram, showing the ages of samples from the Grasberg Igneous Complex arranged in order of decreasing age. Re-Os molybdenite age from Mathur et al. (2005).

skarn formation was linked to potassic alteration of the Dalam intrusive rocks).

Biotite from the medium-grained, equigranular diorite from the Ertsberg Igneous Complex (DZ 5-06 269.3m; Fig. 7D) has been dated at 2.67 ± 0.03 Ma (Table 3), similar to a K-Ar age of 2.65 ± 0.12 Ma for a similar sample dated by McDowell et al. (1996). However, McDowell et al. (1996) also reported ages of 3.00 ± 0.08 and 3.09 ± 0.25 Ma for intrusive rocks from the Ertsberg Igneous Complex, which suggests that at least two ages of intrusions are present.

Phlogopite from an endoskarn vein in the equigranular diorite discussed above has an age of 2.71 ± 0.04 Ma (Table 3), consistent with skarn alteration soon after intrusion of the diorite. Phlogopite from the Ertsberg Cu-Au skarn (Fig. 7H), which is hosted within a roof pendant or screen in the Ertsberg Igneous Complex has an age of 2.59 ± 0.15 Ma (Table 3). This is consistent with a close temporal association between the equigranular phase of the Ertsberg Intrusive Complex and the Ertsberg Cu-Au deposit.

Discussion

Crosscutting relationships between intrusive rocks and hydrothermal veins and alteration, together with ^{40}Ar-^{39}Ar dating of magmatic and hydrothermal biotite from the Grasberg Igneous Complex suggest that the earliest biotite alteration occurred at 3.33 ± 0.12 Ma, while the latest biotite alteration occurred at 3.01 ± 0.06 Ma. The Grasberg chalcopyrite-bornite veins are still younger, possibly having an age similar to the 2.88 ± 0.01 Ma Re-Os age on molybdenite reported by Mathur et al. (2005). Alteration and/or mineralization within the Grasberg Igneous Complex therefore appear to have

occurred over a period of up to 0.5 m.y. but possibly as little as 0.3 m.y. The age of the overprinting high-sulfidation mineralization has not yet been determined.

A close temporal relationship between the main intrusion within the Ertsberg Intrusive Complex, phlogopite in a crosscutting endoskarn vein, and phlogopite from the Ertsberg Cu-Au deposit is apparent from the Ar-Ar data. Re-Os data on molybdenite from Ertsberg gave an age of 2.56 ± 0.02 Ma (Mathur et al., 2005), within error of the Ar-Ar age of phlogopite from the Ertsberg Cu-Au skarn (2.59 ± 0.15 Ma). The Ar-Ar and Re-Os data from Ertsberg together indicate that intrusion and alteration and/or mineralization occurred over a period of 0.1 to 0.2 m.y.

In terms of the temporal evolution of magmatic hydrothermal systems, Grasberg appears to be similar to many other systems where intrusion and alteration and/or mineralization occurred over a period of a few hundred thousand years or less (e.g., Henry et al., 1997; Marsh et al., 1997). Although the Ar-Ar ages reported here range over 0.5 to 0.3 Ma, the relationships between intrusive rocks and hydrothermal veining and alteration at Grasberg indicate that the Grasberg Igneous Complex encompassed several cycles of intrusion and alteration. Dalam and Main Grasberg intrusion stages can be constrained between approximately 3.33 ± 0.12 and 3.19 ± 0.05 Ma, the Kali stage between 3.16 ± 0.06 and 3.06 ± 0.03 Ma, and the Grasberg mineralization stage between 3.06 ± 0.03 and the 2.88 ± 0.01 Ma Re-Os age. This suggests that there were a series of short cycles (≤0.1 m.y.) of structural disruption, intrusion, and hydrothermal veining and alteration. At the broad scale, the Grasberg Igneous Complex formed in a left-lateral strike-slip fault system (Sapiie and Cloos, 2004), but within the Grasberg Igneous Complex itself veining predates nearly all faults (Sapiie, 1998). Early veins are only locally offset by later veins, suggesting that fracturing was largely dilatant in character. This could indicate that fracturing was caused mainly by magmatic and hydrothermal processes in a relatively low-stress regime as proposed by Tosdal and Richards (2001) for porphyry systems elsewhere. Fracturing also could have been facilitated by extension associated with strike-slip faulting (Sapiie and Cloos, 2004) or perhaps by a combination of these processes.

Housh and McMahon (2000) proposed that the isotopic composition of intrusive rocks in the Ertsberg district is consistent with mixing between melts derived from a depleted mantle source with 2 to 3 percent melt derived from an ancient enriched mantle reservoir and interaction with a reservoir characterized by unradiogenic Pb, Sr, and Nd isotope compositions interpreted to be either Archean or Proterozoic lower crustal material. Assimilation-fractional crystallization models were used to suggest a contribution of 10 to 17 percent Archean material or 35 to 75 percent Proterozoic material (Housh and McMahon, 2000). Magmas and fluids which contributed to the formation of intrusions and alteration and/or mineralization in the Ertsberg district appear to have been derived from a deeper seated magma chamber that periodically released magma to form the small, shallow-level intrusions now exposed at the surface. This parental magma chamber may have been replenished at various times during the magmatic-hydrothermal history of the Ertsberg district. For example, Pb isotope evidence from the Ertsberg East skarn system indicates that the ore-forming fluids were derived from a deeper source, which had less crustal contamination than the Ertsberg intrusion (James and Housh, 1995).

The presence of post-Kali diorite intrusions reported here indicates that mafic magma intruded late in the history of the Grasberg Igneous Complex prior to Cu-Au mineralization. In addition, the presence of mafic xenoliths in the Kali intrusions (Pollard and Taylor, 2002) and the Ertsberg intrusion (Katchan, 1982) may be evidence of mingling of basic magma (dioritic) with more felsic magma (quartz monzodiorite) in the deeper magma chamber from which the intrusions were sourced. The different ages of these intrusions determined in this study indicate that mafic input may have occurred at 3.16 Ma (Kali I), 3.06 Ma (post-Kali diorite), and 2.67 Ma (Ertsberg intrusion). This intrusion of basic magmas and possible mingling of basic and felsic magmas may have played a role in mineralization by contributing components such as fluids, metals, and/or sulfur to the ore systems. A key role for synmineralization basic intrusions in supplying sulfur and chalcophile elements for mineralization has been identified at the giant Bingham Canyon Cu-Au deposit (Keith et al., 1998; Hattori and Keith, 2001), and similar processes may have contributed to the huge metal inventory of the Ertsberg district.

Conclusions

Ar-Ar ages of intrusive rocks and hydrothermal infilling and alteration minerals from the Grasberg Igneous Complex range from 3.33 ± 0.12 to 3.01 ± 0.06 Ma. In conjunction with intrusive relationships and paragenetic data they indicate that the Grasberg Igneous Complex encompassed several cycles of intrusion and alteration, each of which persisted for around 0.1 m.y. (and possibly less). These include the Dalam and Main Grasberg intrusion stages between approximately 3.33 ± 0.12 and 3.19 ± 0.05 Ma, the Kali stage, between 3.16 ± 0.06 and 3.06 ± 0.03 Ma, and the Grasberg mineralization stage, between 3.06 ± 0.03 and 3.01 ± 0.06 Ma.

The age of premagnetite phlogopite from the Kucing Liar skarn (3.41 ± 0.03 Ma) is within error of the age of secondary biotite in a fine-grained Dalam intrusive rock (3.33 ± 0.12 Ma). This suggests that skarn formation in the host sediments may have been linked to potassic alteration in Dalam intrusive rocks or possibly an older alteration stage. In contrast, the age of biotite from a skarn on the eastern side of the Grasberg Igneous Complex (3.01 ± 0.06 Ma) is similar to the age of a post-Kali diorite dike. These are both overprinted by Grasberg chalcopyrite mineralization which is probably closer in age to the 2.88 ± 0.01 Ma Re-Os age for molybdenite from Grasberg obtained by Mathur et al. (2005).

Ar-Ar dating indicates that the Ertsberg intrusion and associated alteration and/or mineralization formed at approximately 2.6 to 2.7 Ma and is younger than the Grasberg Igneous Complex intrusive rocks and mineralization. The Grasberg Igneous Complex and Ertsberg data together indicate that there were a series of intrusion and/or alteration systems from around 3.4 to 2.6 Ma, each of which may have lasted for about 0.1 Ma. Evidence of late, mafic intrusive rocks in the Grasberg Igneous Complex and the presence of mafic xenoliths in the Kali and Ertsberg intrusions suggests that these intrusion and/or alteration systems may have been

triggered when mafic magma intruded and mingled with more felsic magma in a deeper magma chamber. Further detailed study of the isotopic evolution of intrusions and hydrothermal fluids in the Ertsberg district may shed more light on the possible role of mafic magmas in providing components such as fluids, metals, and/or sulfur to the ore systems and contributing to the huge metal inventory of the district.

Acknowledgments

The authors would like to acknowledge financial and logistical support from P.T. Freeport Indonesia. PJP and RGT wish to thank the numerous individuals who have helped with our understanding of Grasberg geology and facilitated working in the Ertsberg district. These include Dave Mayes, Chuck Brannon, George MacDonald, Jay Pennington, Imants Kavalieris, Sugeng Widodo, Widodo Margotomo, Al Edwards, and Larry Segerstrom. Widodo Margotomo and Bambang Irawan kindly provided plans and sections illustrating geologic relationships and sample locations, while the final figures were drafted by Jim Austin. Reviews by Mark Cloos, Thomas Bissig, and Dave Cooke resulted in considerable improvement in the clarity of the final version of the manuscript.

August 4, 2004; July 15, 2005

REFERENCES

Clarke, G.W., 2003, Structural and hydrothermal features of the Gunung Bijih Cu skarn deposit, Ertsberg district, Irian Jaya: Townsville, James Cook University, Economic Geology Research Unit Contribution 61, p. 66–73.

Coutts, B.P., Susanto, H., Belluz, N., Flint, D., and Edwards, A., 1999, Geology of the Deep ore zone, Ertsberg East skarn system, Irian Jaya: Australian Institute of Mining and Metallurgy, PACRIM'99, 10–13 October 1999, Bali, Indonesia, Proceedings, p. 539–547.

Deino, A., and Potts, R., 1990, Single crystal $^{40}Ar/^{39}Ar$ dating of the Olorgesailie Formation, southern Kenya rift: Journal of Geophysical Research, v. 95, p. 8453–8470.

Friehauf, K.C., Titley, S., and Soebari, L., 2002, Porphyry-style mineralization in the Ertsberg Diorite, Gunung Bijih (Grasberg) district, West Papua [abs.]: Geological Society of America Abstracts with Programs, v. 32, no. 7, p. 137.

Hattori, K.H., and Keith, J.D., 2001, Contribution of mafic melt to porphyry copper mineralization: Evidence from Mount Pinatubo, Philippines, and Bingham Canyon, Utah, U.S.A.: Mineralium Deposita, v. 36, p. 799–806.

Henry, C.D., Elson, H.B., McIntosh, W.C., Heizler, M.T., and Castor, S.B., 1997, Brief duration of hydrothermal activity at Round Mountain, Nevada, determined from $^{40}Ar/^{39}Ar$ geochronology: Economic Geology, v. 92, p. 807–826.

Housh, T., and McMahon, T.P., 2000, Ancient isotopic characteristics of Neogene potassic magmatism in western New Guinea (Irian Jaya, Indonesia): Lithos, v. 50, p. 217–239.

James, E.W., and Housh, T., 1995, Pb isotopic constraints on the sources of metals in the Gunung Bijih (Ertsberg) mining district, Irian Jaya, Indonesia [abs.]: Geological Society of America Abstracts with Programs v. 27, no. 6, p. A65.

Katchan, G., 1982, Mineralogy and geochemistry of the Ertsberg (Gunung Bijih) and Ertsberg East (Gunung Bijih Timur) skarns, Irian Jaya, Indonesia and the Ok Tedi skarns, Papua New Guinea: Unpublished PhD thesis, Australia, University of Sydney, 498 p.

Keith, J.D., Christiansen, E.H., Maughan, D.T., and Waite, K.A., 1998, The role of mafic alkaline magmas in felsic porphyry Cu and Mo systems: Mineralogical Association of Canada Short Course 26, p. 211–243.

MacDonald, G.D., and Arnold, L.C., 1994, Geological and geochemical zoning of the Grasberg Igneous Complex, Irian Jaya, Indonesia: Journal of Geochemical Exploration, v. 50, p. 143–178.

Margotomo, F.B.W., 2002, Spatial and genetic relationships between silica flooding and main Grasberg quartz stockwork in the southwestern part of the deep Grasberg ore zone, Irian Jaya, Indonesia: Unpublished M.App.Sc. thesis, Townsville, James Cook University, 122 p.

Marsh, T.M., Einaudi, M.T., and McWilliams, M., 1997, $^{40}Ar/^{39}Ar$ geochronology of Cu-Au and Au-Ag mineralization in the Poterillos district, Chile: Economic Geology, v. 92, p. 784–806.

Mathur, R., Titley, R., Ruiz, J., Gibbins, S., and Friehauf, K., 2005, A Re-Os isotope study of sedimentary rocks and copper-gold ores from the Ertsberg district, West Papua, Indonesia: Ore Geology Reviews, v. 26, p. 207–266.

McDougall, I., and Harrison, M.T., 1999, Geochronology and thermochronology by the $^{40}Ar/^{39}Ar$ method, 2nd ed.: New York, Oxford University Press, 269 p.

McDowell, F.W., McMahon, T.P., Warren, P.Q., and Cloos, M., 1996, Pliocene Cu-Au–bearing igneous intrusions of the Gunung Bijih (Ertsberg) district, Irian Jaya, Indonesia: K-Ar geochronology: Journal of Geology, v. 104, p. 327–340.

McMahon, T., 1994a, Pliocene intrusions in the Gunung Bijih (Ertsberg) mining district, Irian Jaya, Indonesia: Petrography and mineral chemisty: International Geology Review, v. 36, p. 820–849.

——1994b, Pliocene intrusions in the Gunung Bijih (Ertsberg) mining district, Irian Jaya, Indonesia: Major and trace element chemistry: International Geology Review, v. 36, p. 925–946.

Meinert, L.D., Hefton, K.H., Mayes, D., and Tasiran, I., 1997, Geology, zonation, and fluid evolution of the Big Gossan Cu-Au skarn deposit, Ertsberg district, Irian Jaya: Economic Geology, v. 92, p. 509–534.

Mertig, H.J., Rubin, J.N., and Kyle, J.R., 1994, Skarn Cu-Au orebodies of the Gunung Bijih (Ertsberg) district, Irian Jaya, Indonesia: Journal of Geochemical Exploration, v. 50, p. 179–202.

Pennington J., and Kavalieris, I., 1997, New advances in the understanding of the Grasberg copper-gold porphyry system, Irian Jaya, Indonesia. Pacific Rim treasure trove: Copper-gold deposits of the Pacific Rim: Toronto, Prospectors and Developers Association of Canada, p. 79–94.

Pollard, P.J., and Taylor, R.G., 2002, Paragenesis of the Grasberg Cu-Au deposit, Irian Jaya, Indonesia: Results from logging section 13: Mineralium Deposita, v. 37, p. 117–136.

——2003, High-sulfidation Cu-Au mineralization in the Ertsberg district, Irian Jaya—implications for genetic models: Townsville, James Cook University, Economic Geology Research Unit Contribution 61, p. 60–65.

Prendergast, K., 2001, Evolution of the West Grasberg breccia zone and gold-bearing limestone breccias; Ertsberg mining district, Irian Jaya, Indonesia: Townsville, James Cook University, Economic Geology Research Unit Contribution 59, p. 168–169.

Rice, C.M., Atkin, D., Bowles, J.F.W., and Criddle, A.J., 1979, Nukundamite, a new mineral, and idaite: Mineralogical Magazine, v. 43, p. 194–200.

Rubin, J.N., and Kyle, J.R., 1998, The Gunung Bijih Timur (Ertsberg East) skarn complex, Irian Jaya, Indonesia: Geology and genesis of a large magnesian Cu-Au skarn: Mineralogical Association of Canada Short Course 26, p. 245–288.

Samson, S.D., and Alexander, E.C., Jr. 1987, Calibration of the interlaboratory $^{40}Ar/^{39}Ar$ dating standard Mmhb-1: Chemical Geology, v. 66, p. 27–34.

Sapiie, B., 1998, Strike-slip faulting, breccia formation and porphyry Cu-Au mineralization in the Gunung Bijih (Ertsberg) mining district, Irian Jaya, Indonesia: Unpublished Ph.D. thesis, University of Texas at Austin, 293 p.

Sapiie, B., and Cloos, M., 2004, Strike-slip faulting in the core of the Central Range of West New Guinea: Ertsberg mining district, Indonesia [abs.]: Geological Society of America Bulletin v. 116, p. 277–293.

Taylor, R.G., 2003, Broken rocks, Breccia 2: Intrusive breccia: Townsville, James Cook University, Economic Geology Research Unit, Ore Textures, v. 5, 52 p.

Tosdal, R.M., and Richards, J.P., 2001, Magmatic and structural controls on the development of porphyry Cu ± Mo ± Au deposits: Reviews in Economic Geology, v. 14, p. 157–181.

Weiland, R.J., and Cloos, M., 1996, Pliocene-Pleistocene asymmetric unroofing of the Irian fold belt, Irian Jaya, Indonesia: Apatite fission-track thermochronology: Geological Society of America Bulletin, v. 108, p. 1438–1449.

Widodo, S., Manning, P., Wiwoho, N., Johnson, L., Belluz, N., Kusnanto, B., MacDonald, G., and Edwards, A., 1999, Progress in understanding and developing the Kucing Liar orebody, Irian Jaya, Indonesia: Australian Institute of Mining and Metallurgy, PACRIM '99, Bali, Indonesia, 10–13 October, 1999, Proceedings p. 499–507.

APPENDIX

Sample preparation and irradiation

Mineral separates were prepared using standard crushing, dilute acid treatment, and handpicking techniques. Mineral separates were loaded into a machined Al disc and irradiated for 7 h in the D-3 position, Nuclear Science Center, College Station, Texas. Neutron flux monitor Fish Canyon Tuff sanidine (FC-1). Assigned age = 27.84 Ma (Deino and Potts, 1990) relative to Mmhb-1 at 520.4 Ma (Samson and Alexander, 1987).

Instrumentation

Samples were analyzed with a Mass Analyzer Products 215-50 mass spectrometer on line with an automated all-metal extraction system. Mineral separates irradiated in samples NM-98, NM-115, NM-133, and NM-148 were step-heated, using an Mo double-vacuum resistance furnace. Heating duration in the furnace was 7 to 9 min. Reactive gases were removed during furnace analysis by reaction with three SAES GP-50 getters, two operated at ~450°C and one at 20°C. Gas was also exposed to a W filament operated at ~2,000°C. Mineral separates were irradiated in sample NM-123 step-heated with a 50-W CO_2 laser using a beam integrator lens. Heating duration was 3 min. Reactive gases were removed by reaction with two SAES GP-50 getters, one operated at ~450°C and one at 20°C. Gas was also exposed to a W filament operated at ~2,000°C.

Analytical parameters

Electron multiplier sensitivities were as follows: 1.0 ?10^{-16} mol/pA, sample NM-98; 1.65×10^{-16} mol/pA, sample NM-115; 1.47×10^{-16} mol/pA, sample NM-123; 3.05×10^{-16} mol/pA, sample NM-133, and 1.70×10^{-16} mol/pA, sample NM-148. Total system blank and background averaged 686, 37, 1.5, 1.5, 2.3×10^{-18} mol at masses 40, 39, 38, 37, and 36, respectively. J factors were determined to a precision of ±0.1 percent by CO_2 laser fusion of four single crystals from each of 4 radial positions around the irradiation tray. Correction factors for interfering nuclear reactions were determined using K glass and CaF_2 and are as follows: $(^{40}Ar/^{39}Ar)_K$ = 0.0002 ± 0.0003; $(^{36}Ar/^{37}Ar)_{Ca}$ = 0.00028 ± 0.000005; and $(^{39}Ar/^{37}Ar)_{Ca}$ = 0.0007 ± 0.00002.